

Axisymmetric Parachute Shape Study

Vladimir S. Drozd¹

Airborne Systems North America, Santa Ana, CA, 92704, United States

Parachute inflated shape is one of the main parameters that drives parachute performance in steady descent. This paper looks at axisymmetric parachute shape formation, particularly the relationship between parachute constructed geometry, number of gores, gore shape, pressure distribution and inflated parachute shape. Stresses in a parachute structure are discussed in relation to parachute inflated shape. Analytical estimates derived from one dimensional parachute model are extended by a finite element analyses performed with LS DYNA software.

Nomenclature

A_0 - canopy reference area, nominal

N - number of canopy gores,

S_m - length of the canopy radial from an apex to a skirt

$s = S / S_m$ - dimensionless distance from apex to a current point along the radial

$x, y = X(s), Y(s) / S_m$ - dimensionless x, y coordinate of a radial point

\vec{n} - unit vector in plane of the radial and normal to the radial

$\vec{\tau}$ - unit vector tangent to the radial

$2a$ - distance between the radials on inflated canopy

r - fabric strip arch local radius

R - distance from the canopy centerline to the radial along the normal \vec{n} to the radial

γ - fabric strip arch half angle

l - inflated gore half length (gore arch half length)

α - half angle between the adjacent radial normal vectors

φ - angle between a tangent to the radial and X-axes

F - confluence force

q - dynamic pressure

$p = p(s) / q$ - dimensionless pressure distribution along radial

C_p - pressure coefficient,

C_d - drag coefficient

C_c - carrying capacity coefficient

T - tensile force in a radial,

$Ft(s)$ - tangential distributed force component along the line,

$Fn(s)$ - normal distributed force component along the line,

T_f - distributed tensile force in a fabric strip,

L - lines length

Dimensionless parameters are used as follows:

¹ Systems Analyst, Space and Recovery Systems, 3000 Segerstrom Avenue, Santa Ana, CA 92704 USA.
AIAA Member

$$T = \bar{T} \cdot q \cdot S_m^2$$

$$F_n = \bar{F}_n \cdot q \cdot S_m$$

$$F_t = \bar{F}_t \cdot q \cdot S_m$$

$$s = \bar{s} \cdot S_m$$

The dashes above the dimensionless values are omitted in a text below

Introduction

Demanding and changing performance requirements to modern parachute systems keep up continual interest to new parachute designs and improvements of the existing systems. The broad spread of today's requirements vary from a single use cargo delivery system where cost is likely a design driving factor to a space recovery systems where chute performance per unit of system mass is often a major efficiency criteria.

Industry advances in textile materials and new parachute assembly methods enhanced with modern simulation techniques open additional opportunities in satisfying today's rigorous requirements, often allowing engineers to take another look at already existing concepts and consider a new ones.

Despite seemingly being around forever and studied thoroughly circular parachutes are not an exclusion, and on the contrary prove time over time their necessity and superiority for many existing and new applications.

Mostly experimental approach of early days to a parachute design provides engineers with valuable factual data of parachute performance. Today those data can be complimented by advancements in parachute simulation methods. Achievements in a finite element analyses (FEA) and fluid structure interaction (FSI) allow for simulation of the real life structures with acceptable accuracy and more and more realistic outcomes, parachutes not being an exclusion. Quickly growing computing power makes simulation results also feasible within a reasonable computing time.

FSI methods by their definition involve coupling of fluid and structure motions and therefore represent the most advanced and adequately complex approach to a parachute behavior analyses.

On the other hand FEA method thoroughly considers structural part of parachute behavior, provided distributed aerodynamic loads applied to a parachute surface are known. In some cases those loads may be available from experiments or estimated separately, which allows structural analyses of parachute to be complete.

As universal computational methods FSI and FEA methods are applicable to any type of a parachute structure provided parachute geometry is known.

Being very powerful in their ability to analyze local effects (like stress concentrations for complicated shapes for example) on another hand they do not provide that analyses convenience compared to the cases when system behavior can be described and analyzed through analytical relationships between major design defining parameters.

Fortunately a circular parachute has some specific construction features that allowed researchers to come up with a relatively simple and meanwhile productive parachute structural model.

Circular parachute canopy structure consist of radials forming vertical wire frame, and a fabric segments filling space between the radials, fig. 1 (A horizontal circumferential reinforcing is present quite often as well). This schematic of a circular parachute closely matches the pathway the loads are distributed in a canopy structure and transferred to the confluence point.

Due to a fabric curvature a distributed pressure load $p(s)$ normal to the canopy surface get transformed into a tensile load T_f in a fabric. Tensile loads in a fabric in turn get transferred as a distributed loads to the radials. Eventually radials collect distributed load and transfer it to the lines.

Since a radial is a linear flexible element the radial shape and a tension T in a radial can be described by flexible line equations:

$$dT / ds = -Ft(s) \quad (1)$$

$$d\varphi / ds = Fn(s) / T \quad (2)$$

$$dx / ds = \cos(\varphi) \quad (3)$$

$$dy / ds = \sin(\varphi) \quad (4)$$

Where

- T - tensile force in a radial,
- s - linear coordinate along the radial

$Ft(s)$ - tangential distributed force component along the radial,
 $Fn(s)$ - normal distributed force component along the radial,
 φ - angle between a radial curve tangent and X-axis ,
 x, y - rectangular coordinates of the radial point

This approach has been used successfully to simplify the case and produce a model that adequately describes a static structural loading of the circular parachute in many important cases. The concepts of the model have been implemented in CANO and later in CALA codes for a circular parachute structural analyses [1].

Although aimed primarily to determine structural loads in a canopy for known constructed geometry and a pressure distribution, the developed parachute model and corresponding equations provide a valuable tool for a circular parachute shape study.

Canopy loading

Major assumptions of the model deal with the question of *how* the load comes from a canopy fabric to the radials. It is assumed that fabric itself is a one dimensional structure consisting of a set of independent circumferential elements (ribbon parachute is a good example). Actual solid cloth parachute falls into that category when radial strains (stresses) in a fabric are negligible, compared to the circumferential ones.

Since pressure along the fabric strip element is considered constant, the fabric strip takes a shape of a circle arch of angle $2 \cdot \gamma$ between two attachment points to the adjacent radials.

Due to an assumed absence of structural interference between fabric strips the value of tensile load T_f in them are statically determined when pressure $P(s)$ and the fabric strip radius of curvature r are known.

In general case a radial is not perpendicular to the plane of a fabric strip, therefore a tensile force \vec{T}_f applied from a fabric strip to a radial may have both along the radial component $Ft(s)$ and a normal to the radial component with projection $Fn(s)$ in plane of the radial.

These components may be approximated by the following dimensionless expressions :

$$Fn(s) = 2 \cdot p \cdot x \cdot \sin\left(\frac{\pi}{N}\right) \cdot \frac{\sin(\gamma - \alpha)}{\sin \gamma} \quad (5)$$

$$Ft(s) = -2p \cdot x \cdot \sin^2\left(\frac{\pi}{N}\right) \cdot \frac{\cos(\gamma - \alpha)}{\sin \gamma} \cdot \frac{\cos \varphi}{\cos \alpha} \quad (6)$$

Equilibrium equations (1-2) and geometrical relationships (3 - 4) form enclosed system of differential equations for four unknown functions $x(s), y(s), T(s), \varphi(s)$ and known boundary conditions. With XY reference system origin being at canopy apex the boundary conditions are:

$$\varphi(s = 0) = 0, \quad \text{and} \quad (7)$$

$$\varphi(s = 1.0) = \varphi_m \quad (8)$$

where φ_m is the radial angle at the point of line attachment.

When right sides of the equation (1-2) are known the equations can be integrated numerically. However pressure distribution along the radial is not known in advance (coupling problem, mentioned before), what makes the case open.

Nevertheless there is still a certain reason in studying solutions of equations (1-4). Available experimental data of pressure distribution around the canopies (including various shaped canopies and solid models) give some idea of pressure distribution along the radial and a range of pressure variation. Given that it is possible to run some parametric studies without knowing the exact pressure distribution.

Since forces developed by a parachute depend in part on its inflated shape, and mainly on its projected area, it seems to be important to keep a projected area at its maximum for a given constructed dimensions. For a given constructed radial length only a gore width distribution differ one solid cloth canopy design from another (provided fabric permeability and lines length remains the same for all designs).

Historically canopy shape evolved from a flat circular to a conical, and then to a more complicated quarter spherical and extended skirt designs. That evolution resulted in a canopy gore width decrease compared to a flat circular gore. Fig.2 shows gore material distribution in each of them for a 30 gore canopy. Since flat circular canopy has the widest gore does it also produce the maximum possible inflated diameter for a given constructed diameter? Is it possible to increase a canopy inflated diameter by adding more material into the gore? In general, how does a material distribution in a gore control a canopy inflated shape?

Some observations about the canopy shape can be made based on the structure of the equations describing a radial loading

Free shaped (pressure shaped) parachutes

Figure 1 shows canopy schematic and the components $F_n(s)$, $F_t(s)$ of the distributed load applied to the radial. Beside a pressure function both of these components (5-6) contains two angles: α and γ . Angle $2 \cdot \alpha$ is an angle between the normals of the adjacent radials. It is determined by number of the gores in a canopy and by a position along the radial. Thus angle α describes a radial geometry and can be expressed as

$$\alpha = \arcsin\left(\sin\left(\frac{\pi}{N}\right) \cdot \sin(\varphi)\right) \quad (9)$$

Angle α varies along the radial and has its maximum value of $\alpha = \pi/N$ at the maximum inflated canopy diameter ($\varphi = \pi/2$) For a typical 30 gore canopy it is in a range of $0 \leq \alpha \leq 6^\circ$.

On another hand fabric strip arch angle γ indicate a gore material fullness at a particular point along the radial which may be characterized by a ratio of a fabric strip arch length l over the distance a between the radials at the point of consideration:

$$l/a = \gamma / \sin \gamma \quad (10)$$

Theoretically a range of possible angles γ may vary from 0 (no fullness in a canopy) to a $\gamma - \alpha = \pi/2$ when gore has maximum fullness.

This particular case is a subject of interest. In this case as it seen from (5-6), $F_t(s) = 0$ Physically it means that tensile force in a fabric strip lies in plane of the radial and is perpendicular to the radial, thus not having a component in a direction along the radial. As a result a tensile force T in a radial remains constant all the way along the radial which formally results from eq.1.

It is reasonable to expect a small variation of tensile radial force for the cases when angle $\gamma \gg \alpha$ still.

On the other hand for $\gamma \gg \alpha$ normal to the radial force component $F_n(s)$ does not change a lot as well. That means a radial shape is not going to change substantially with angle γ variation provided angle γ is high. Since angle γ is a measure of a gore fullness, it is expected that canopies with a lot of gore fullness all have a similar radial shapes.

Based on the features of available fullness it is convenient to call these class of canopies a free shaped parachutes. For these parachutes their shape is controlled by a pressure distribution (or rather a presence of pressure difference at the canopy surface, since shape itself is almost independent of a pressure distribution itself)

Shaped parachutes

Free shape parachutes are those where $\gamma \gg \alpha$ at any point along the radial. Opposite to this case is the case when $\gamma = \alpha$. That makes

$$F_n = 0, \text{ and } d\varphi/ds = 0 \quad (11)$$

In this case angle φ remains constant and the following condition must be met:

$$\sin(\gamma) = \sin\left(\frac{\pi}{N}\right) \cdot \sin(\varphi) \quad (12)$$

Apparently, canopies with constant φ along a certain part of the radial resemble the conical surface shape at that area. The shape of the conical part of the canopy does not depend on a pressure distribution along the conical part of the canopy, but rather is determined by a geometry of the gore.

For a small φ angle γ is also small and may be approximated as

$$\gamma = \varphi \cdot \frac{\pi}{N} \quad (13)$$

Thus knowing (or assigning desirable) angle φ , a variety of conical canopies with different cone angles can be generated. Knowing angle φ , and the number of gores N, all other canopy parameters are determined for the area where $\varphi = const$

$$a = x \cdot \sin\left(\frac{\pi}{N}\right) \quad (14)$$

$$l = x \cdot \sin\left(\frac{\pi}{N}\right) \cdot \frac{\gamma}{\sin(\gamma)} \quad (15)$$

Angle φ can not remain constant all the way along a radial since at the line attachment point it must be higher than 90 degrees to satisfy boundary conditions. Consequently a transition area from a conical to different shape is required. Since in this area angle φ must change substantially, angle γ deviates from angle α to produce a required F_n .

Theoretically the conically shaped parts of the canopy may exist at any φ , even when φ is greater than 90 degrees (at skirt area) provided there is a positive pressure difference across the canopy shell in this area. In this case a general equation (12) must be used to obtain angle gamma for this part of the canopy.

When “ conical “ load conditions are met at the cylindrical part of the canopy it experiences hoop stresses only. Cylindrical part of the canopy has another interesting feature. The angle $\varphi = \pi/2$ for a cylindrical part of the canopy (maximum diameter of the inflated canopy area). Therefore in accordance with eg. (1,6) tensile force in a radial must remain unchanged along the radial at that areas of the canopy regardless of gore fullness.

Thus there are two ultimate cases of canopy shapes – free shaped, or pressure shaped parachutes, and a shaped parachutes, where canopy shape in certain areas is determined purely by a gore geometry. In between those ultimate cases a general expression (5-6) must be used when integrating system of equation (1-4) for angle φ .

Tension in a canopy fabric.

Tension in a fabric strip is given by the expression

$$T = r \cdot p = a \cdot p / \sin(\gamma) = x \cdot p \frac{\sin\left(\frac{\pi}{N}\right)}{\sin(\gamma)} \quad (16)$$

It become evident again the importance of angle γ (or fullness in a canopy gore). The more fullness in a gore is, the less is the tension in a canopy fabric. In a conical canopies circumferential stresses therefore are higher than stresses in a free shaped canopies.

Pressure distribution approximation

Since governing equations are not going to be solved for the exact pressure distributions, some reasonable pressure distribution approximations are used. Linear pressure distribution along the radial is perhaps the simplest one to consider

$$P(s) = q \cdot m + k \cdot q \cdot s / S_m = q(m + ks / S_m) = Cp \cdot q \quad (17)$$

The first constant term “m” is used to characterize say “average” pressure acting on a canopy surface, or pressure at some characteristic point along the radial, say at canopy apex or close to it. The second term “k” describes pressure variation along the radial.

The following range of pressure parameters was considered:

$$m = \{ 0.5 - 1.4 \}, \quad k = \{ 0.0 - 0.5 \} \quad (18)$$

Gore geometry parameters

As it was discussed earlier a pressure distribution is not the only parameter that controls the solution of governing equations describing canopy shape. Expressions (5-6) for distributed forces contain an angle γ - a parameter that characterizes a gore fullness distribution along the radial. It is convenient to use this parameter

instead of a gore width. When $\gamma \gg \alpha$ then canopy has a lot of gore fullness. When $\gamma - \alpha \sim 0$ then canopy does not have any fullness in a gore. These special cases were touched above giving an idea of canopy shape for them. The intermediate cases require solution of the governing equations.

As a first step a system of equations was integrated for a range of angles γ and linear pressure distribution. A relative lines length ratio $L/S_m = 2$ was used as a typical value. Fig.3 shows the respective computed radial shapes for a range of angles γ , while gore width distribution along the radial for various angles γ is shown in fig. 4. As it is seen from fig.3 a maximum gore fullness provides maximum canopy inflated diameter. A substantial decrease in a gore fullness (decrease in angle γ from 90 degrees to ~ 30 degrees) does not lead to a drastic decrease in an inflated diameter, but substantially decreases a gore width.

Fig.5 and 6 show tension distribution in the radial itself and in a fabric material respectively. It may be seen that the radial's tension remains the same for a wide gore, but starts changing when gore fullness drops. The radial tension change is not pronounced at the skirt of the canopy area, where canopy has close to a cylindrical shape, as it was discussed earlier.

Similarly to a parachute drag coefficient Cd a canopy efficiency can be estimated by a carrying capacity coefficient Cc defined as $Cc = F/q \cdot A$. Carrying capacity coefficient is not a truly drag coefficient since it is based on a prescribed pressure distribution, but would converge to a drag coefficient for a correct pressure distribution. Fig. 7 presents change in the Cc coefficient with the angle γ for two considered pressure distributions - constant ($m=1, k=0$) and a quasi linear pressure distribution shown in fig. 3. The canopy inflated radius is also plotted in fig.7 for both pressure distributions. Both sets of curves help to explain the trend in changes of the carrying capacity curve.

The canopy inflated dimension very lightly depends on the pressure distribution pattern. The increase in the inflated canopy radius varies from 4 to 2 % with pressure change, which tells that canopy inflated diameter almost insensitive to a pressure distribution pattern.

An increase in a canopy inflated radius is only $\sim 5\%$ when angle γ changes from 30 to 90 degrees. This leads to a certain observation about inflated parachute canopy shapes. Since angle γ determines canopy gore width distribution along the radial, all canopies having their gore width distribution curve above the "border" line curve for $\gamma = 30^\circ$ must have their shapes enclosed between blue and green lines in fig.3 In this respect, their inflated radial shape is not very sensitive to the gore width distribution. Thus all the canopies satisfying that condition must look very alike in terms of their radial shape when inflated. Charts fig.7 also show that canopy inflated radius decreases sharply at small angles γ .

As it may be seen the carrying capacity coefficient Cc reaches its maximum within a certain range of angles γ . At high angles γ the coefficient Cc goes down due to an increase in a gore fabric area. This increase in a gore fabric area is not supported though by the adequate increase in a canopy projected area.

At low angles γ canopy inflated radius drops sharply thus driving down canopy carrying capacity.

A comparison of gore width distributions for various but constant angles γ in fig.4 shows that none of them matches a flat circular canopy gore width distribution. A flat circular gore width distribution is closely approximated by angle $\gamma \sim 30$ degrees at small distance s along the radial (apex area), but has a lot of fullness at the skirt area. Much better match is achieved with use of a variable angle γ , as shown in fig.8. Despite an increase in the angle γ at the skirt, an extra material at the skirt area resulted in a decrease of the carrying capacity coefficient Cc from 0.63 to a 0.60.

FEA results

One-dimensional parachute model discussed above emphasized important relationships and geometry parameters responsible for canopy shape formation. Some important canopy shapes have been discussed.

More detailed canopy shape and fabric stress analyses requires two dimensional fabric model. It was done using a FEA simulation for a several gore shapes using a commercial LSDYNA software[5].

Rectangular gore.

Parachute design that utilizes a simple solid cloth rectangular strip of fabric as a gore was studied during a low cost parachute design project. Being unique in a construction itself this design is also a good example to be used in a simulation.

As an example the simulation was done for the canopy having a radial of 5.5 m long and 30 gores.

A gore width “w” was considered as a variable parameter, and a series of simulations was performed for each fixed gore width. Same as before pressure parameters “m” and “k” have been varied within the range $m = \{ 0.5 - 1.4 \}$, $k = \{ 0 - 0.5 \}$ to simulate various pressure distribution scenarios and their influence on a canopy shape. A summarized results of the simulations are presented in fig.9 – 11.

As it can be seen from charts fig.9 inflated canopy radial radius stays almost the same when gore width decreases from its maximum value, and then suddenly begin to decrease when gore width drops below a certain value. Physically that effect is directly related to the gore fullness decrease with the gore width decrease, Fig.10. Gore fullness decrease does not influence substantially load $F_n(s)$ applied to the radial up to a certain moment, so as a it does not influence a radial loading, and consequently canopy shape (radius remains almost unchanged). When gore fullness becomes small, then situation sharply getting changed in an area of small fullness. Now with the width decrease canopy mouth radius decreases proportionally. Comparison of curves for radius change shows that radius change with pressure change disappears as soon as width dropped below critical value. So canopy inflated diameter is almost invariant to a pressure distribution change along the surface, (which also have been discussed earlier).

Cc coefficient

The Cc charts presented in Fig. 9. show distinctive maximum at certain gore width. The Cc increase with the initial gore width decrease is explained by a decrease in a reference area for a Cc calculation, not by an increase in a confluence force. As it is shown in Fig.11 the actual confluence force F drops with gore width decrease (canopy mouth diameter stays the same, but fullness drops, so does the mouth area). But the actual rate of reference area decrease is higher than a rate of a force decrease, so a Cc is going up.

On the contrary, the confluence force drop after the bend at $w=0.4$ is mainly the result of canopy mouth diameter change. In this area of $w<0.4$ m a force drops faster than a reference area does.

Fabric stresses.

Fabric stress distribution in a gore for 2 rectangular gore canopy designs are shown fig 22-23 and plotted in chart Fig. 10. This chart also clearly indicates change in a canopy behavior. Basically circumferential stresses jumped from one level to another level as soon as gore width value passed through critical region of $w=0.4$ m. Low stresses at the right part of the chart represent local stresses in a bulged between the radials fabric. High stresses at the left part of the chart in turn represent “hoop” stresses in a cylindrical part of the canopy formed when gore width dropped below critical region.

This last situation has $F_n = 0$, and therefore $d\phi/ds = 0$. So canopy shape in this area takes a cylindrical shape with virtually no gore fullness ($\gamma = \alpha$ condition). Circumferential fabric tension in this area may be estimated as $T = r \cdot p$ And for $r = 3.6$ m, $p = 90$ N/qs.m, $T = 3.6 \cdot 90 \cdot 0.1 \cdot 2.2 \cdot 0.0254 = 1.83$ lb/inch. For comparison LS Dyna computed circumferential tension is $T = 1.94E-6 \cdot 4E+6 \cdot 0.1 \cdot 2.2 = 1.8345$ lb/inch

Triangular gore shape.

Triangular gore shapes historically are associated with a flat circular canopy, having triangle angle at apex $\beta = 2 \cdot \pi / N$. So called conical chutes have that angle $\beta \leq 2 \cdot \pi / N$, with narrower gore. Nothing prevent though to consider the gore shapes having gore angle larger than $\beta = 2 \cdot \pi / N$, which is, in a way, similar to a rectangular gore with extra fabric discussed before.

As an example for the FEA a canopy having a radial of 5.5 m long and 30 gores have been considered. In this case a conical gore shape was simulated. A gore width at apex was fixed to a reasonably small value 0.02 m convenient for simulation purposes. A gore width “w” at canopy skirt was considered as a variable parameter, and a series of simulations was performed for each fixed gore width. As before, pressure parameters “m” and “k” have been varied within the range $m = \{ 0.5 - 1.4 \}$, $k = \{ 0 - 0.5 \}$ to simulate various pressure distribution scenarios.

A summarized results presented below in charts fig.12 – 15. for $m=1$, $k=0, 0.5$

As it can be seen from charts Fig.12 canopy inflated dimension (characterized by radial radius) stays almost unchanged between $w = 0.53 - 0.6$ m, and then slowly decreases when gore width drops. The same results are presented in Fig. 13 vs cone angle. It is seen that canopy inflated diameter stays practically constant up to cone

angle 30 degrees, and then start decreasing. Physically that effect is again directly related to the gore fullness decrease with the gore width decrease. The difference between a rectangular gore and a triangular gore lies in what canopy part that fullness becomes close to 1.0 first.

In case of a rectangular gore that happens first in the area of the maximum canopy diameter, and then progresses up along the radial, see pictures of gore shapes in fig.16-21.

In case of a triangular gore that happens first in an intermediate area (due to a certain fullness given in the apex area), and then progresses down the gore and up the gore when gore angle decreases (cone angle increases, in terms of standard terminology). In those areas radial takes the shape of a straight line (a condition of $\frac{d\phi}{ds} = 0$ discussed earlier). A computed inflated gore shapes and stress distribution in them are presented in fig. 24-28 for a range of cone angle 0-45 degrees.

It is important to note that up until this, say critical, angle range of ~ 30 degrees is reached, canopy shape (radial shape) is the same as the one for a rectangular gore, or any other shaped gore. They all have one thing in common – they all have sufficient gore fullness and therefore behave identical in terms of canopy shape forming, - like a free shaped parachutes. From that standpoint a flat circular, and all coned parachutes having cone angle less than 30 degrees will not look like a cones when inflated, but rather will look like a regular flat circular in terms of their radials spatial shape. Experimental results on 20 degrees conical canopy testing may be found in [2]

When gore fullness became small in the case of a rectangular gore, it is immediately influenced canopy mouth dimension. With the width decrease canopy mouth radius decreased proportionally.

Not the same is in case of the conical chutes. Absence of fullness, or say, fabric deficiency in a gore leads to an increase of the cone angle.

Same as before, comparison of curves for radius change (Fig.12-13) shows that radius change with pressure change becomes less noticeable with cone angle increases. So canopy inflated diameter is almost invariant to a pressure distribution change along the surface, (which also have been discussed earlier).

Cc coefficient

The Cc charts presented in Fig. 12-15 show an area of widths (cone angles) where parachute Cc reaches maximum and remains almost unchanged. This happens at 28-42 degrees cone angle. Same as it was in the case with a rectangular gore, the Cc increase with the initial gore width decrease (cone angle increase) is explained by a decrease in a reference area for a Cc calculation, not by an increase in a confluence force. Similar results reported in [3,4]. Fig.14 shows that the actual confluence force F drops with gore width decrease (canopy mouth diameter stays about the same, but fullness drops, so does the mouth area). But an actual rate of reference area decrease is higher than a rate of a force decrease, so the Cc is going up.

Fairly flat Cc curve between 28-42 degrees reflects the fact of force decrease due to a proportional mouth diameter decrease.

Further increase in a cone angle shows drop both in a Cc and a confluence force.

So what cone angle is the optimal one in a canopy design if Cc is constant within a range of angles? Apparently some other than Cc factors must be taken into account.

Typically chute performance is characterized by a canopy Cc which involves canopy surface area as a denominator. By default canopy surface area is often associated with a chute total mass. In reality a canopy fabric mass is about 30% of total chute mass, especially for the systems with long lines and risers. So 10% in surface area increase will give 10% of fabric mass increase, but only 3-4% of total parachute mass increase. In an extreme case, when fabric weight is negligible compared to a total parachute mass, we will be actually looking at the force generated by parachute of the fixed diameter and line lengths. For this reason it is make sense to look at the force a canopy generates, and use this force as a second criteria. In our case of conical canopy force drops continuously with a cone angle increase, Fig.15. So for this reason the more efficient chute will be the one with 28-30 degrees angle since it generates higher force that chute with say 45 degrees angle.

Canopy shape optimization considerations

As it was shown above a rectangular gore shape has a lot of fullness at large gore width, which does not really contribute to a drag producing. When a gore width decreases and reaches a certain value where the gore fullness drops substantially, canopy inflated diameter decreases, and performance start suffer. With a rectangular canopy that fullness drop happens in a lower canopy portion (skirt area). The best canopy carting capacity coefficient was found to be right at that transition zone of gore width or slightly above it. As it was shown a growth of carrying

capacity coefficient with a gore width decrease is mainly a result of fabric area decrease, without a change in a radial spatial shape (canopy shape and inflated canopy diameter).

This observation suggest a natural approach to parachute efficiency improvement . As a first step gore width at any point along the radial can be brought down to the point where it will start influence canopy inflated diameter. With this approach canopy shape will not be influenced, but canopy fabric area will be decreased.

A further fullness elimination in canopy top area theoretically must lead to a conically shaped areas of the canopy. Conically shaped canopy seems to be attractive to study with an aim to flatten the radial curvature and decreasing a size of a “vertical canopy wall”, thus potentially opening canopy mouth.

It is important to notice that the above considerations are based on the assumption of the same pressure distribution for all the shapes considered. Despite it was shown that pressure distribution (its value, and a pressure variation along the radial only slightly change canopy shape), the actual drag coefficients for particular canopies will be dependent on actual pressure values. So the results above should not be used for estimating actual drag coefficients, but for a relative comparison in between various shapes.

Therefore the above results may be used for a preliminary canopy shape choice, and must be supported at the next stage by FSI analyses. Fig.29-30 show an example of some results of FSI analyses. Comparison between simulation and experimental results for different canopy shapes is complicated by observed in simulations breathing of some canopies and therefore an absence of a steady state condition, accurate account for a canopy permeability and actual canopy geometry.

References

1. New Solution Method for Steady-State Canopy Structural Loads. W.D.Sundberg. Jornal of Aircraft, 1988
2. SAND77-705 Pressure and profile data of 20 degrees conical ribbon parachutes. H.G.Heinrich , J.I.Uotila. University of Minnesota . Technical report, 1977
3. Parachute Recovery Systems Design Manual. T.Knacke, NWC TP 6575, 1992
4. Recovery Systems Design Guide. AFFDL-TR-78-151
5. LS-DYNA keyword user’s manual, May 2007. Livermore Software Technology Corporation (LSTC)

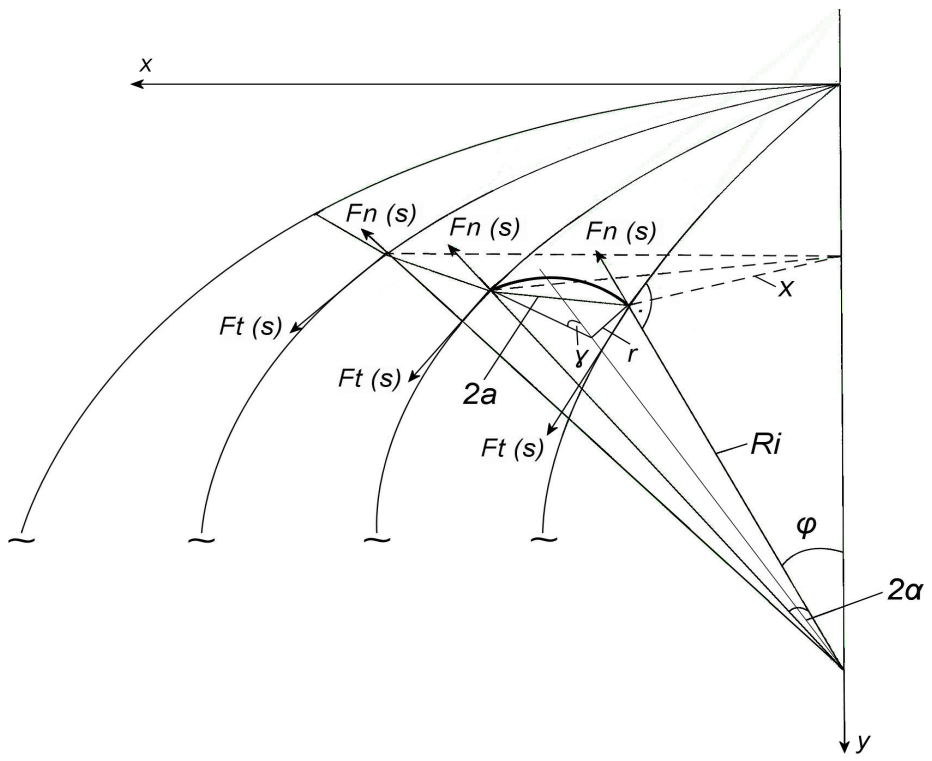


Fig.1

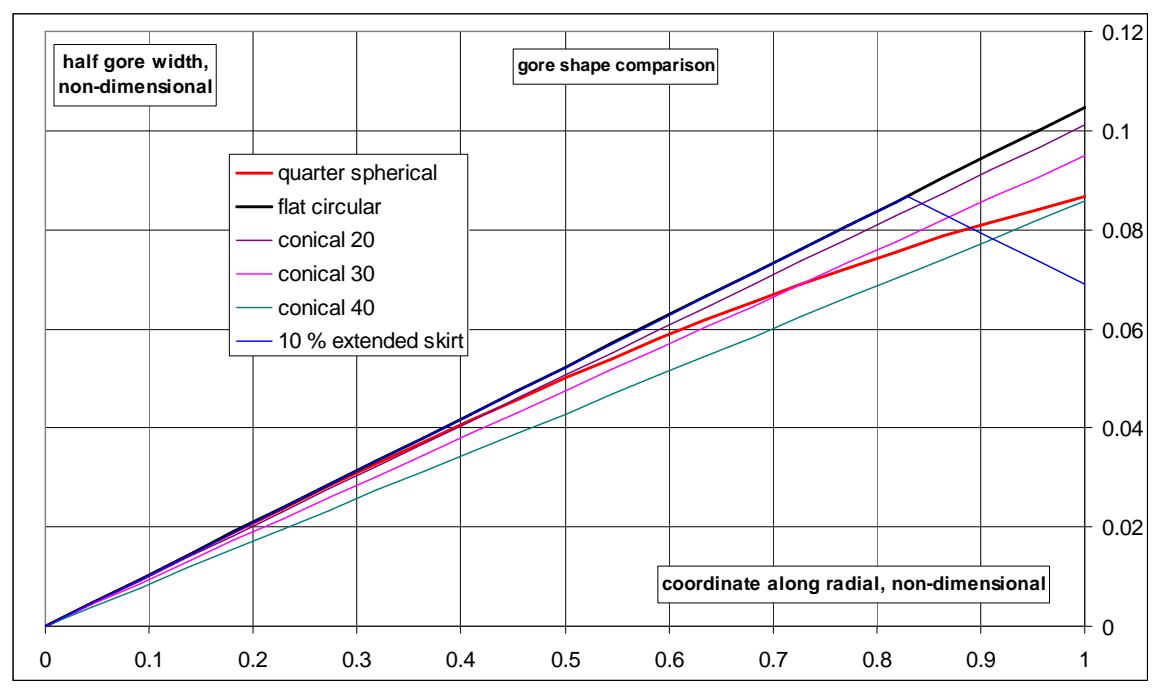


Fig. 2

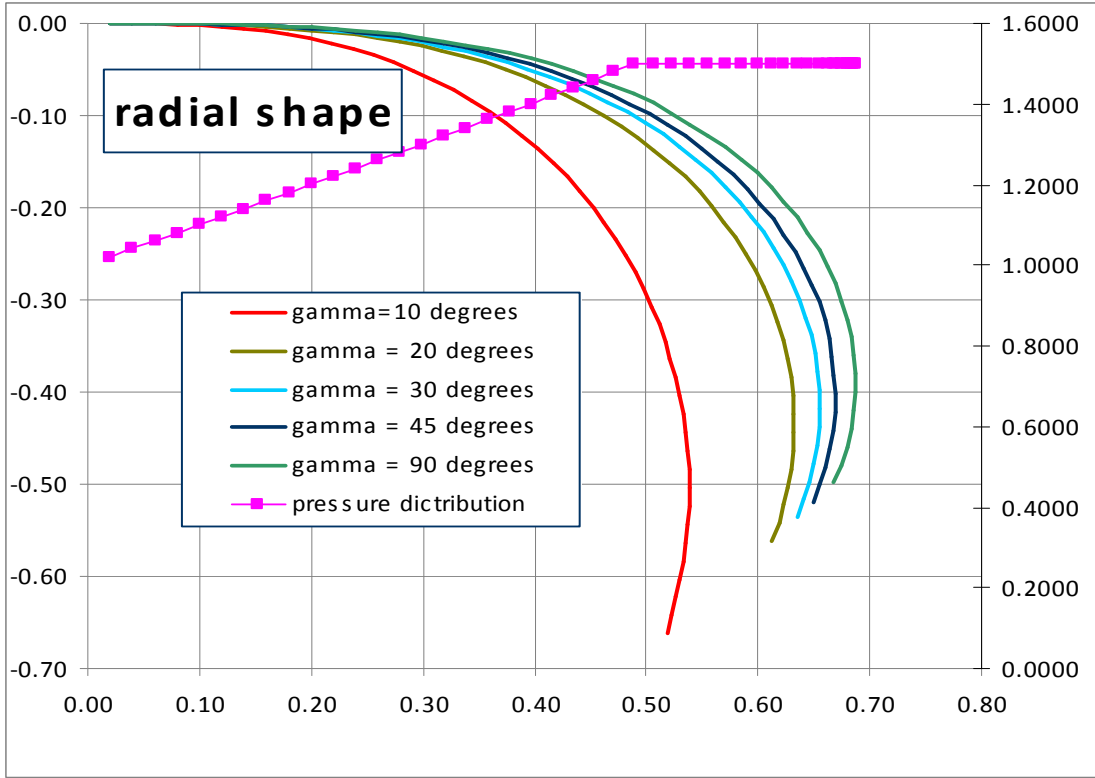


Fig.3

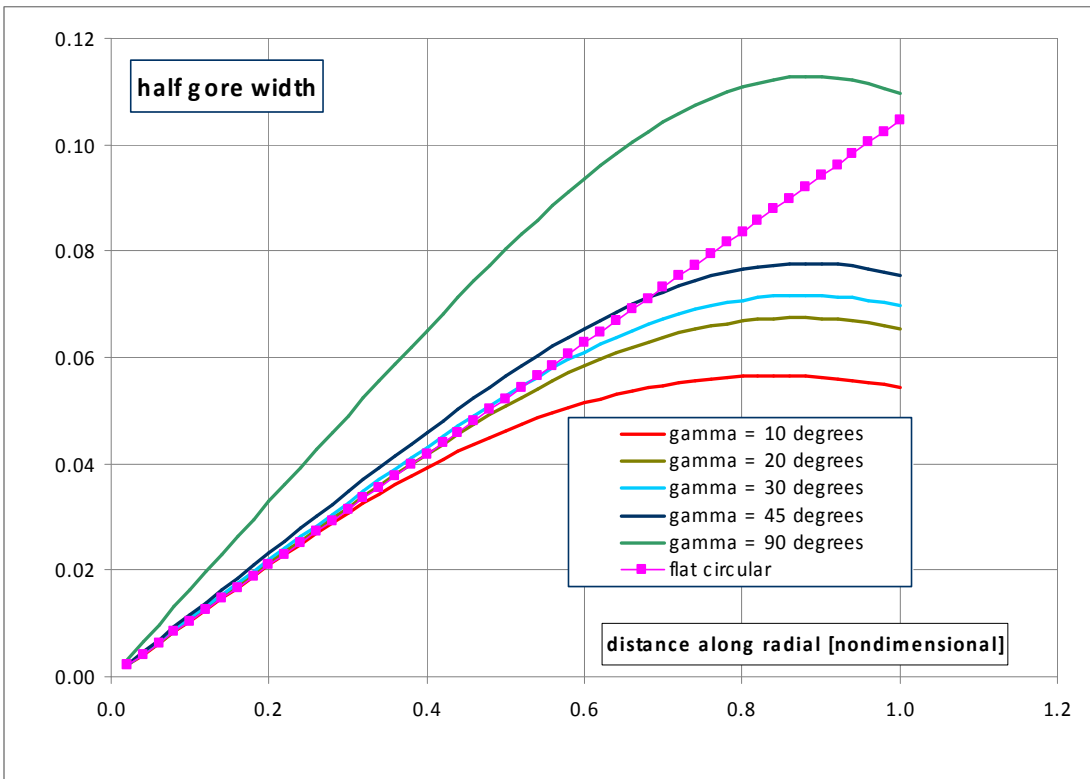


Fig.4

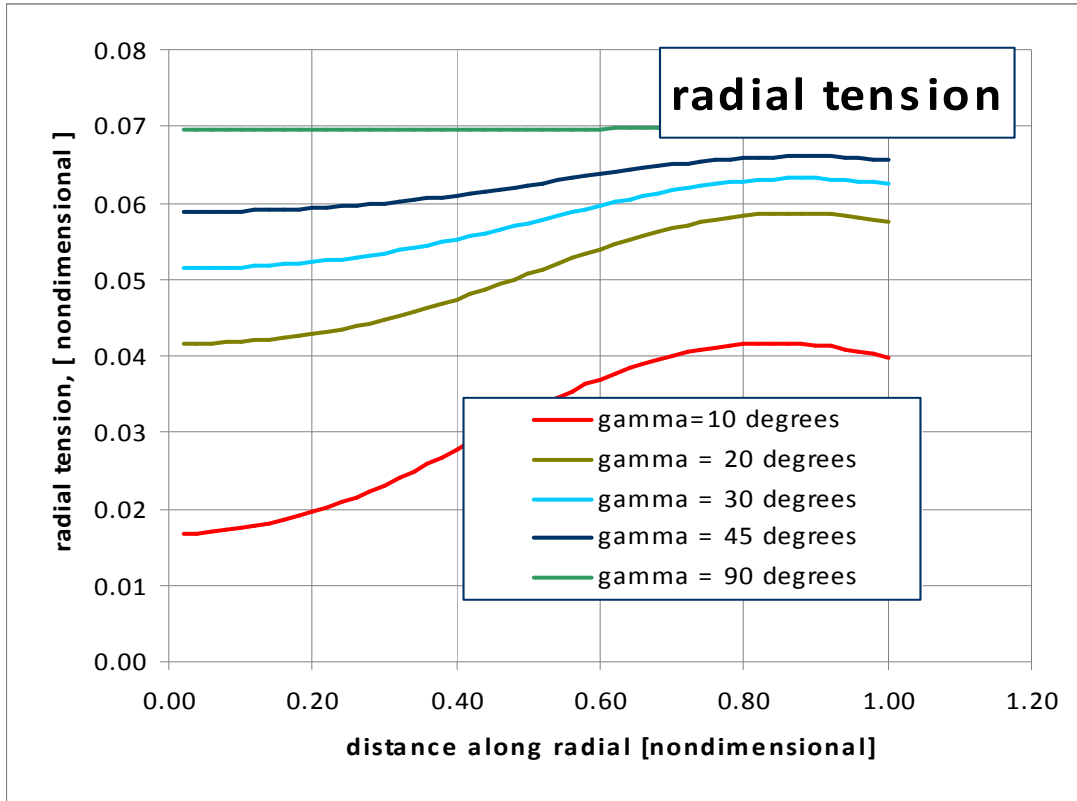


Fig. 5

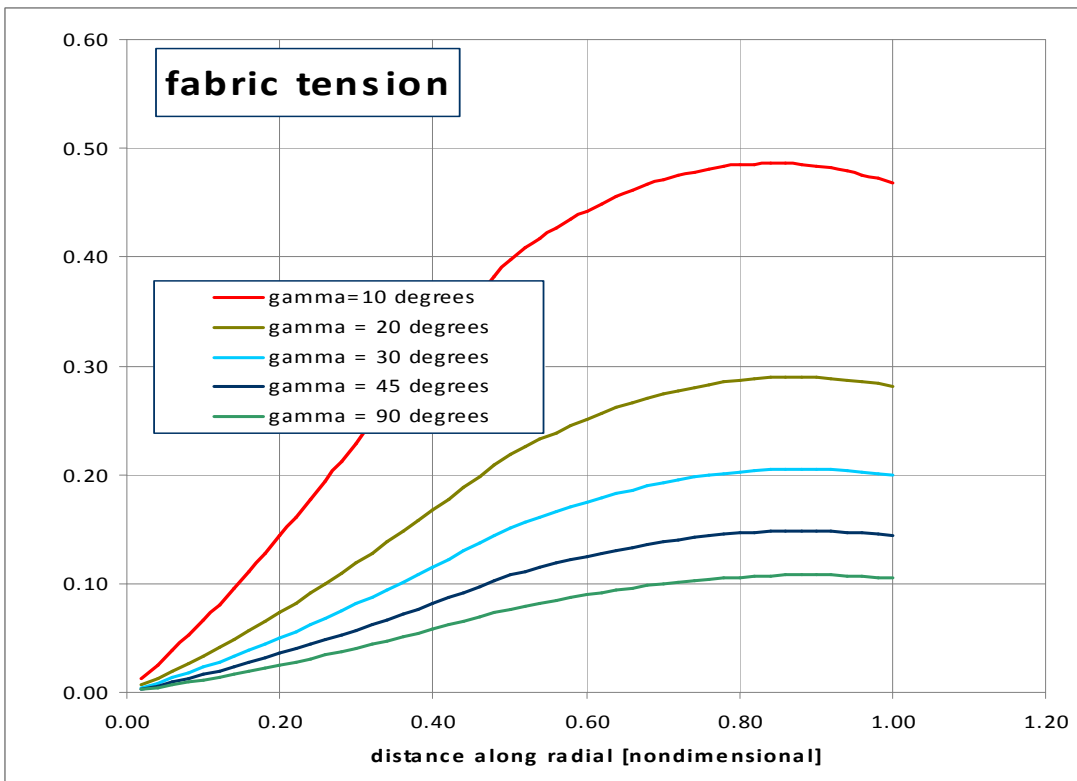


Fig. 6

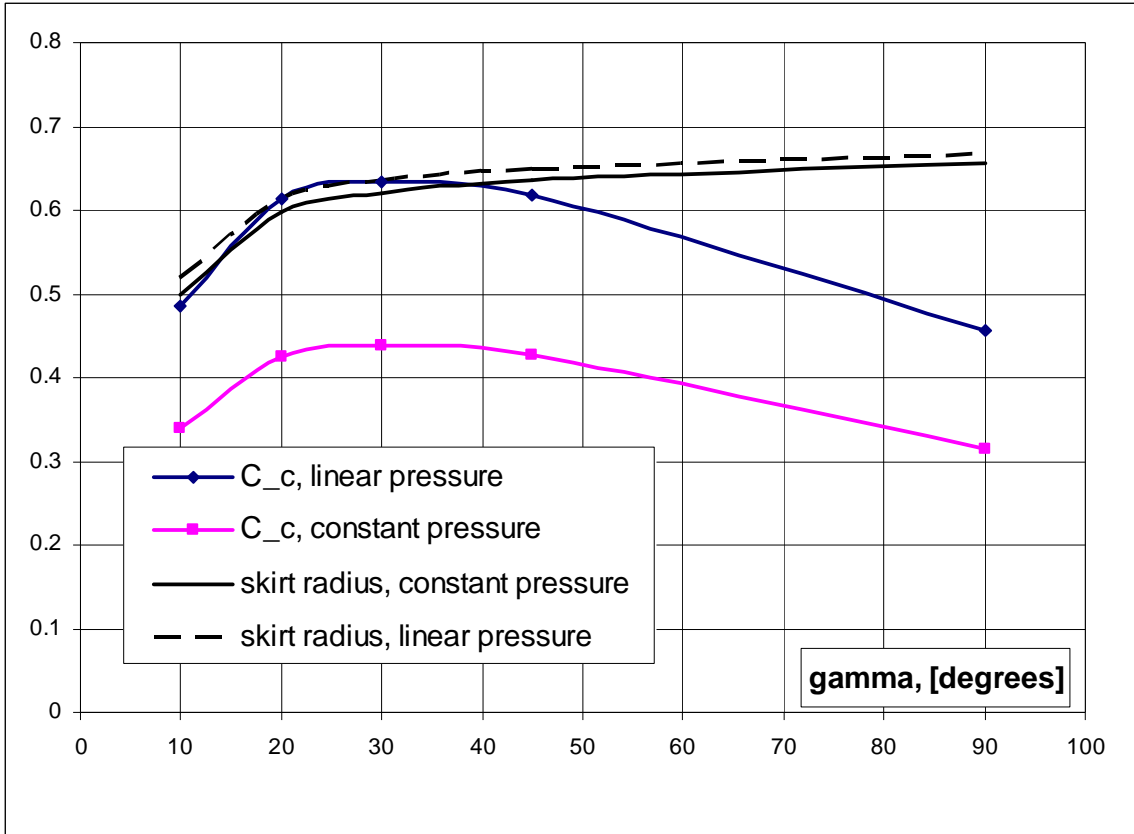


Fig. 7

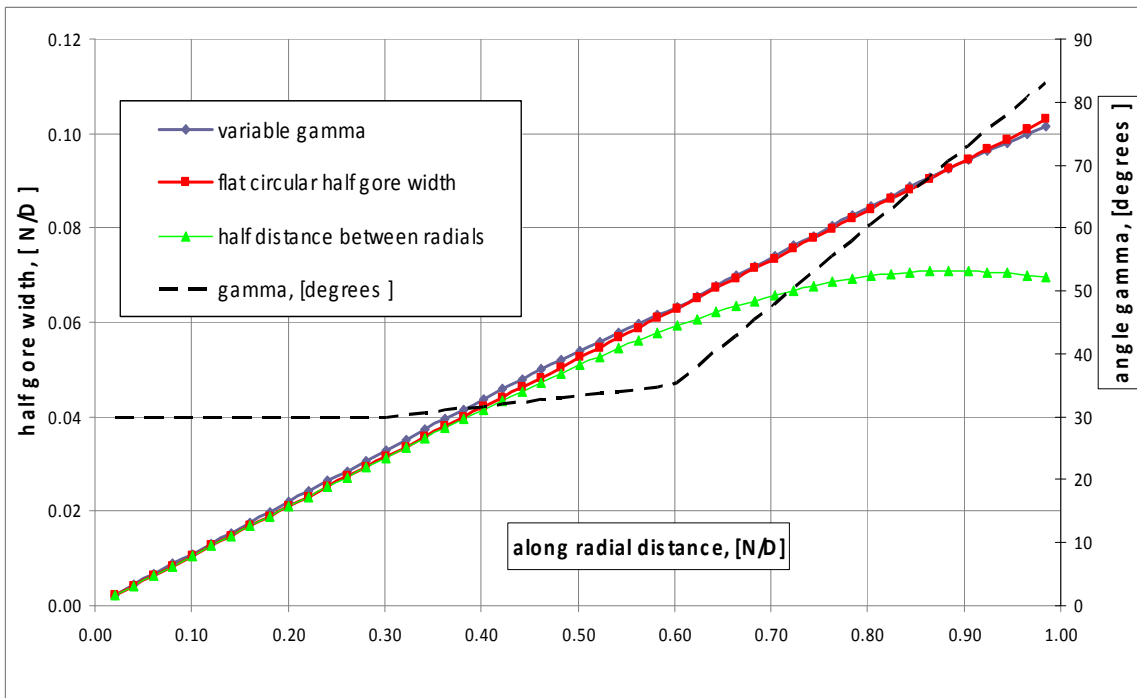


Fig. 8

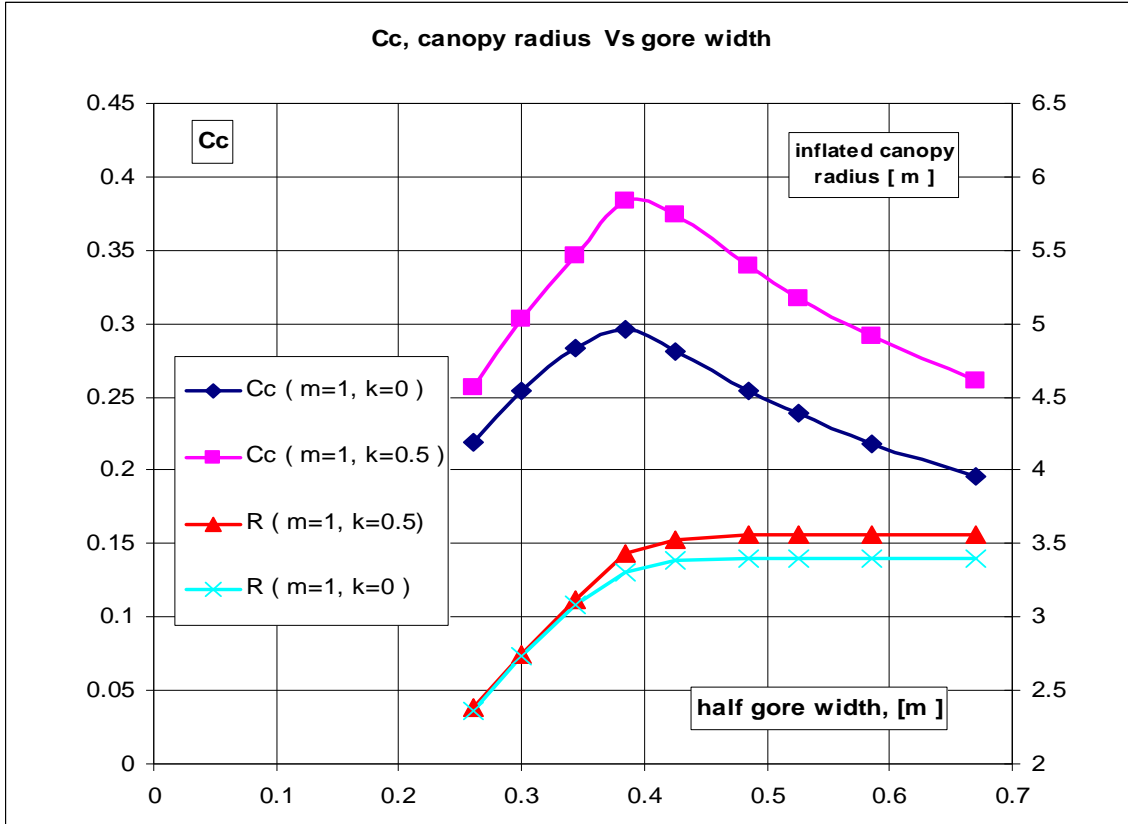


Fig. 9

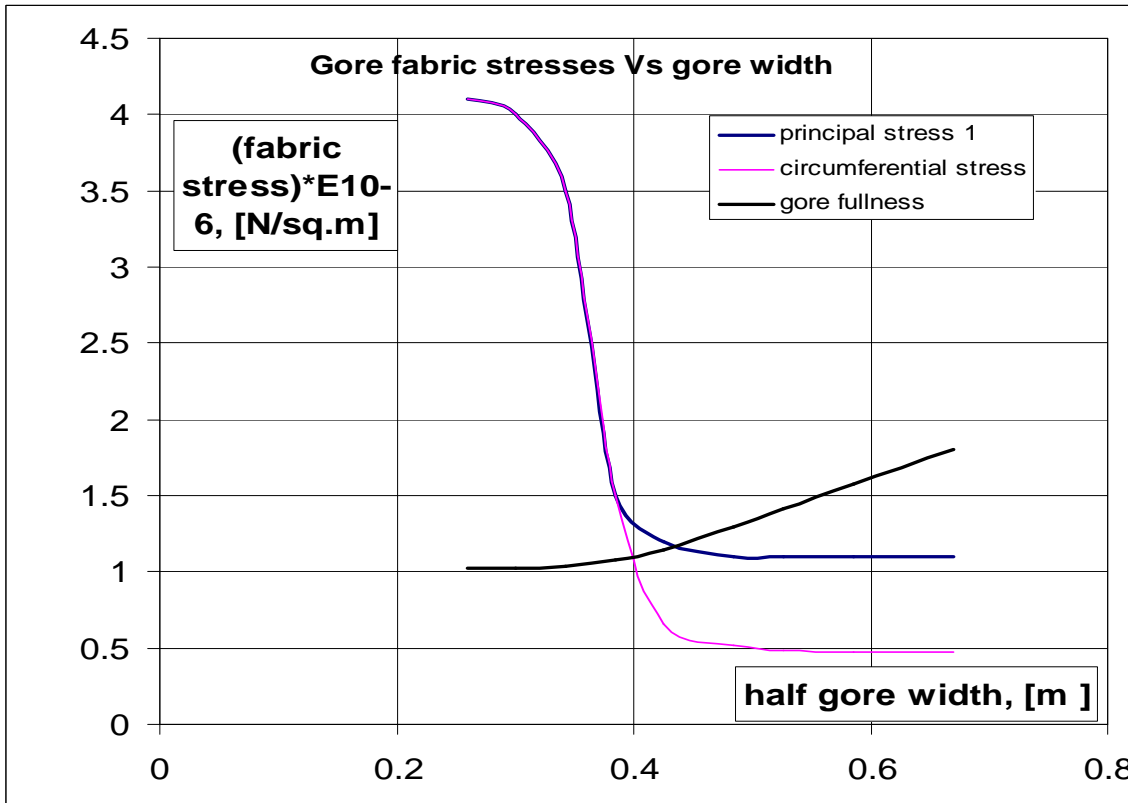


Fig.10

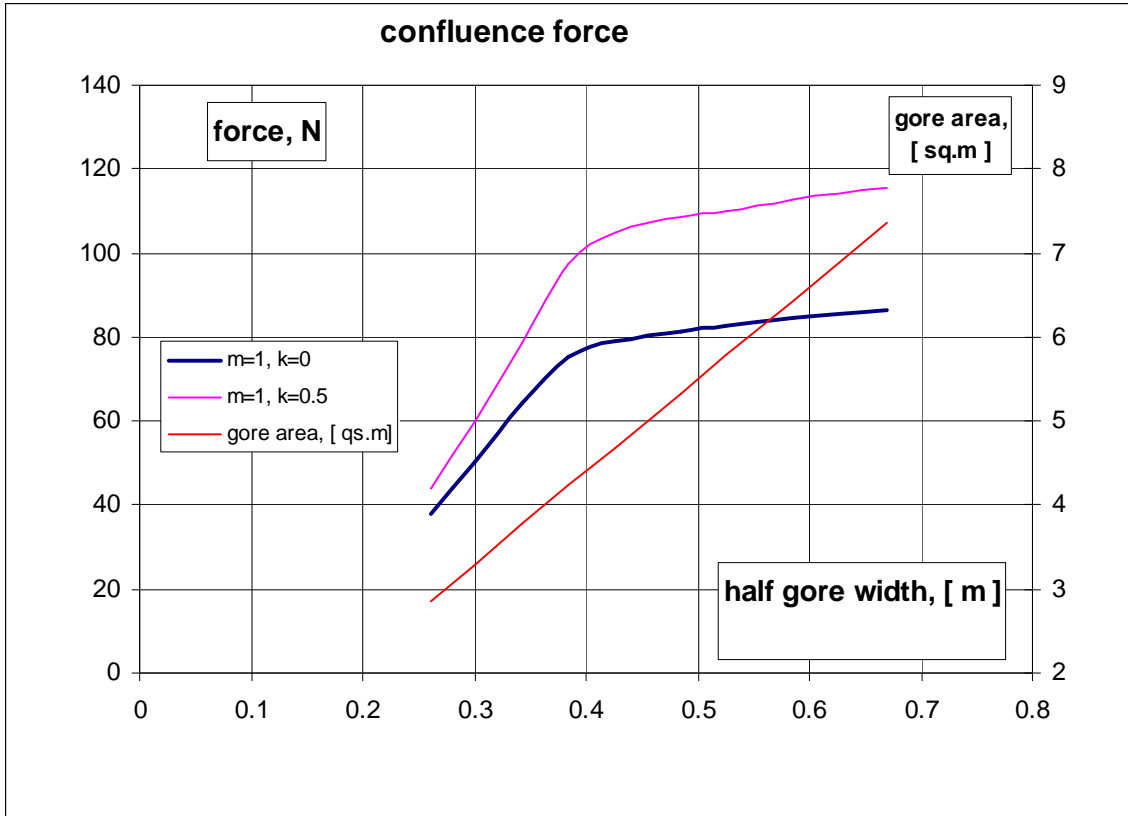


Fig.11

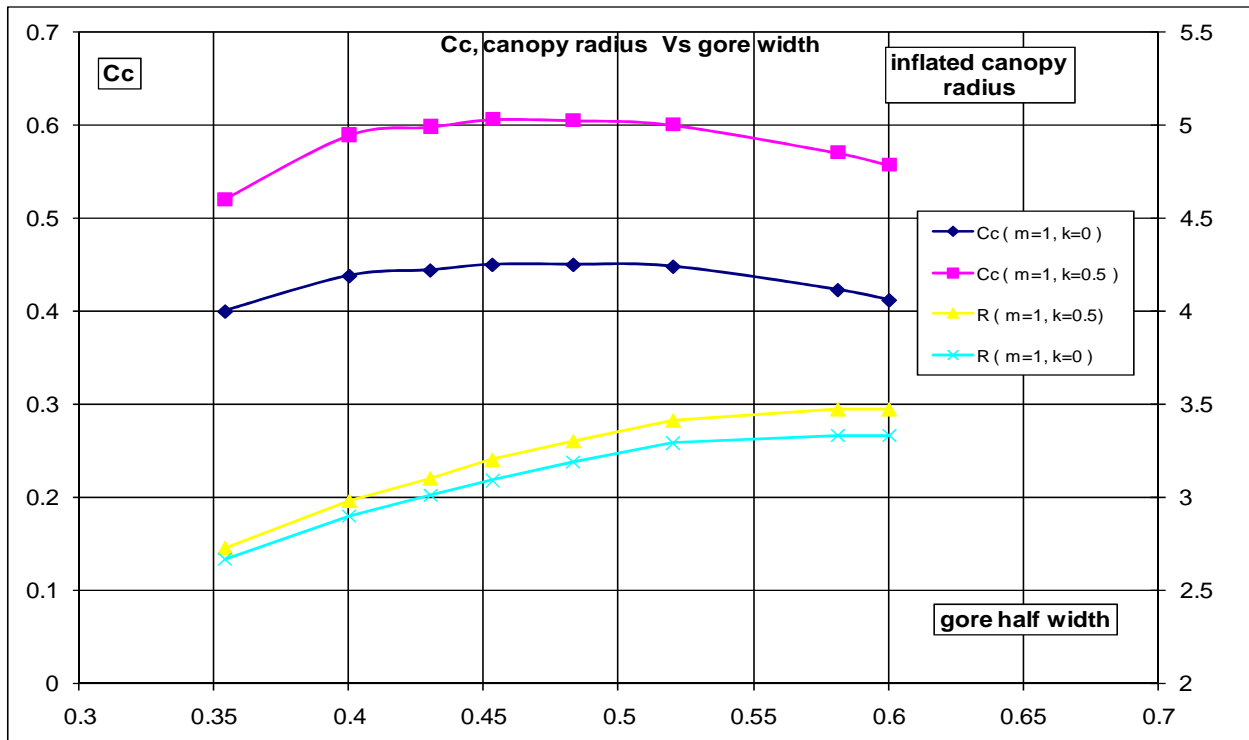


Fig. 12

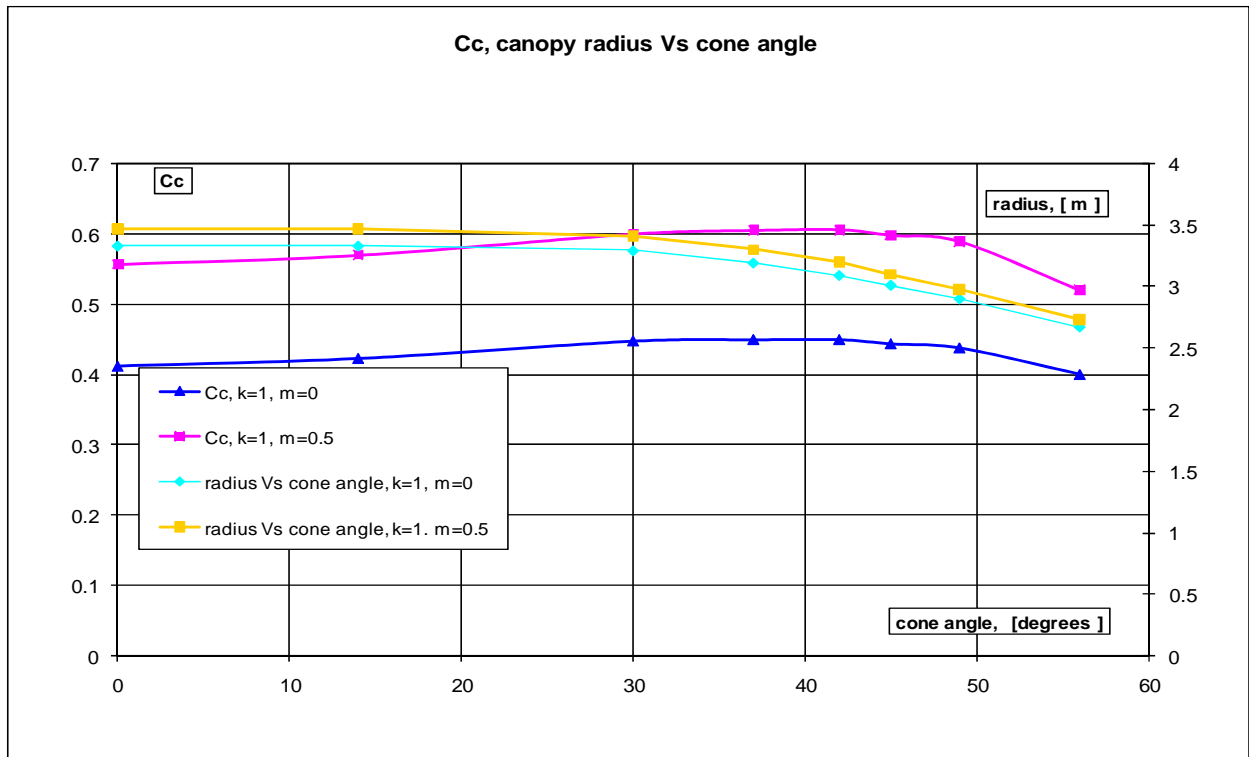


Fig. 13

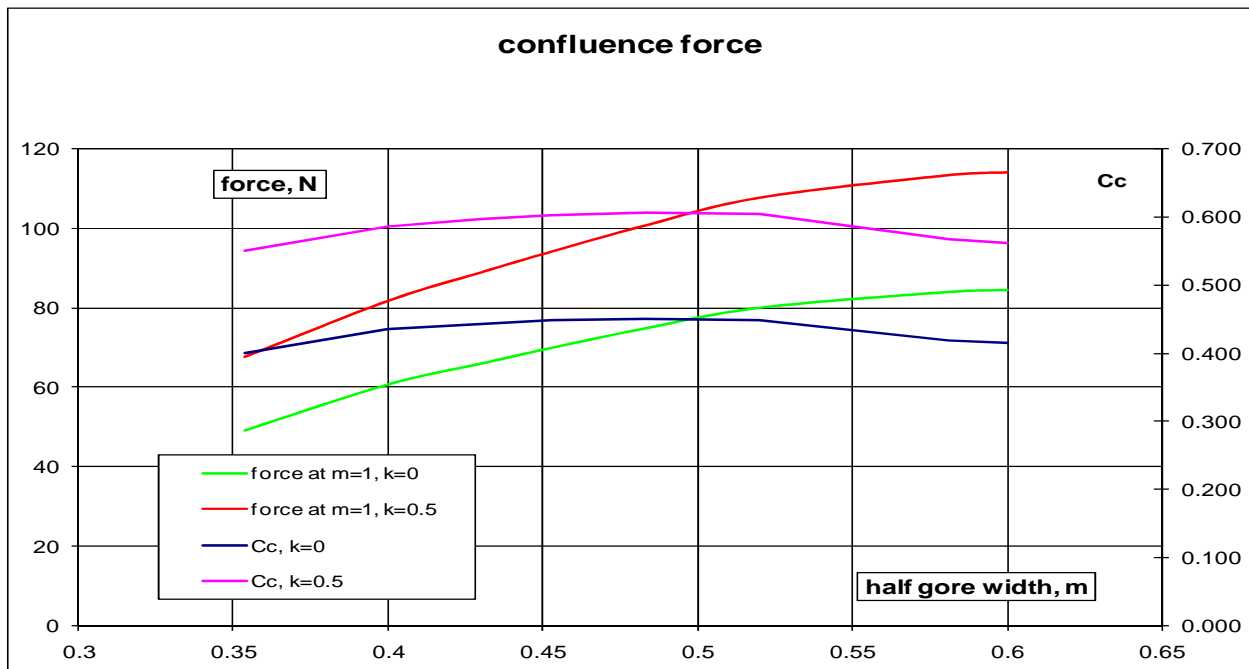


Fig.14

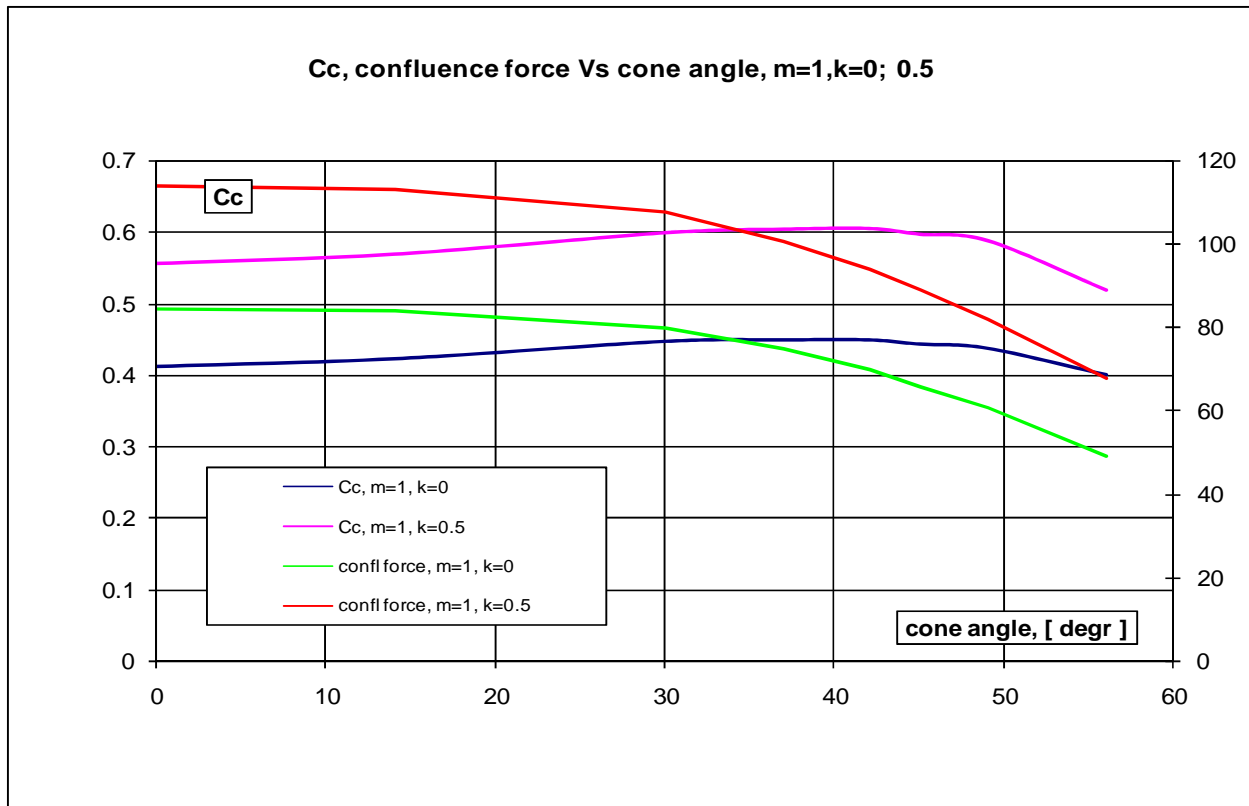


Fig.15

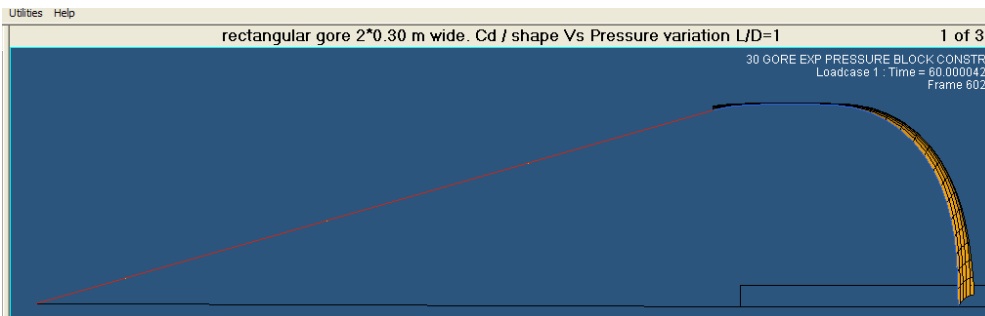


Fig. 16

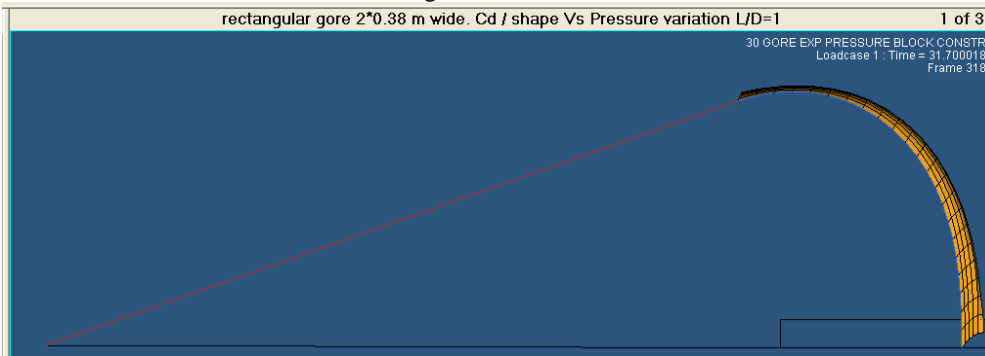


Fig.17

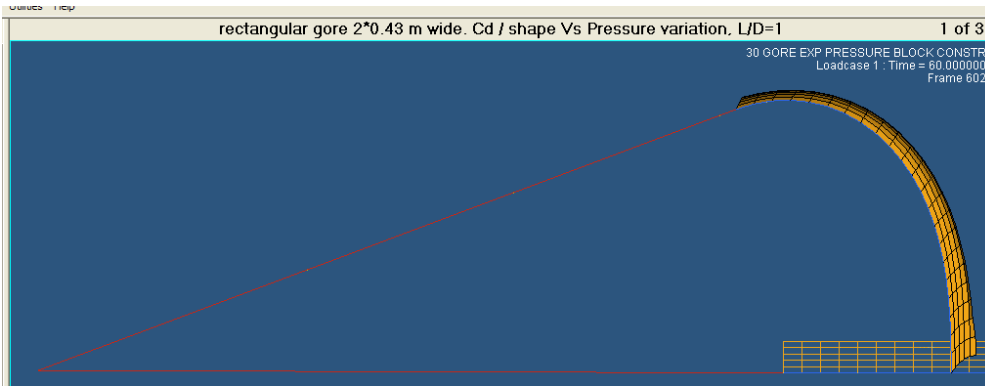


Fig.18

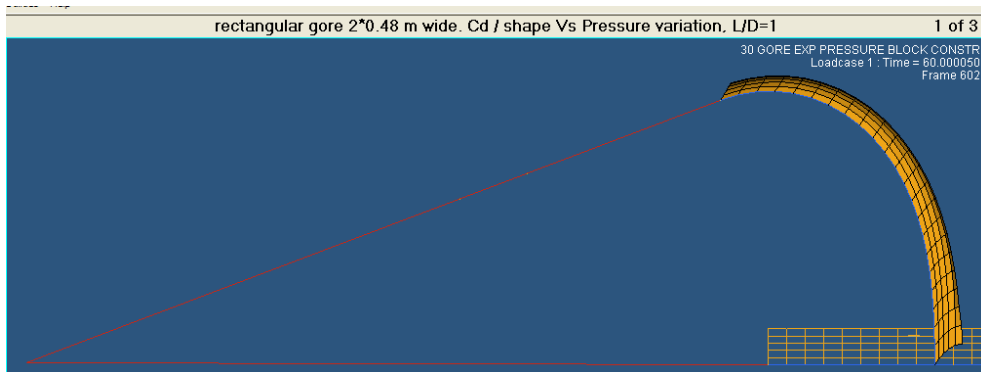


Fig.19

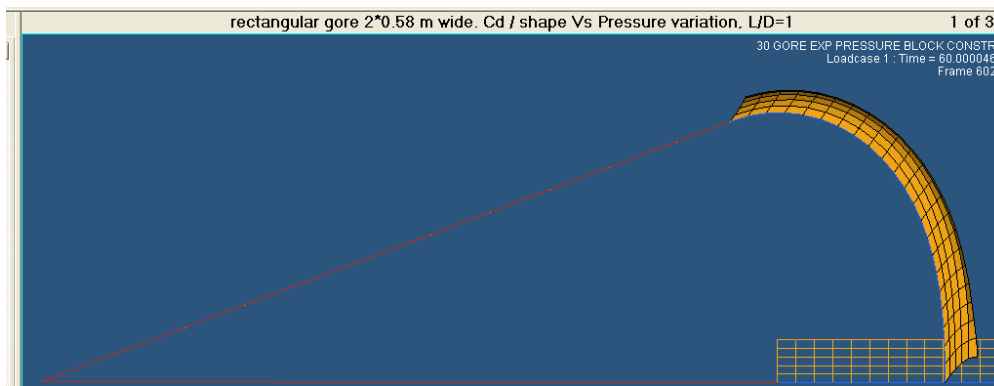


Fig.20

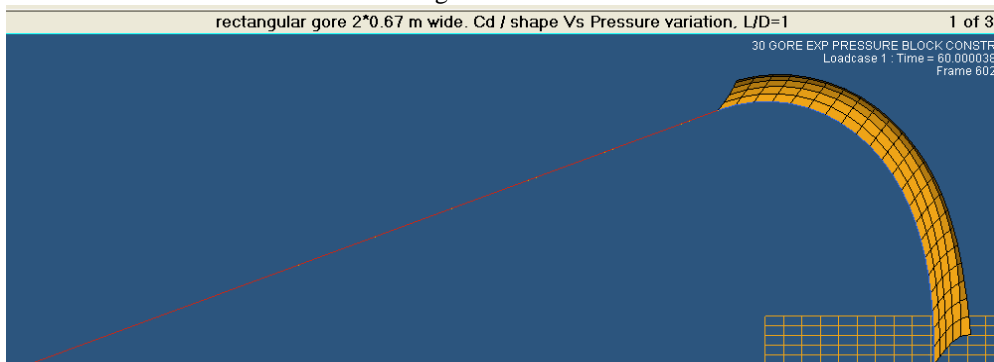


Fig.21

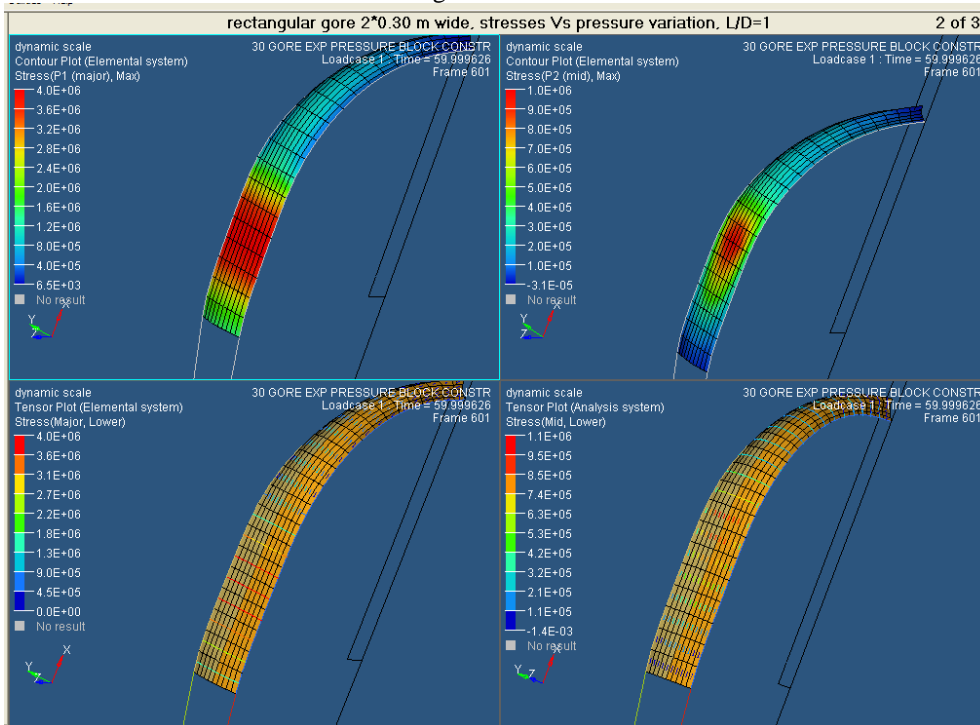


Fig.22

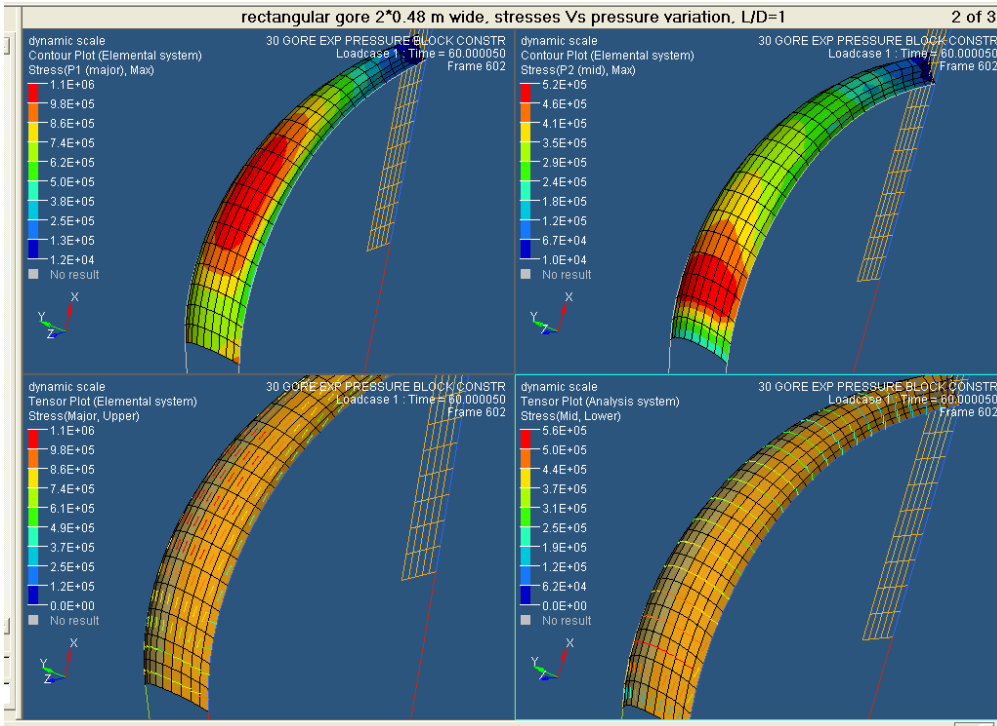


Fig.23

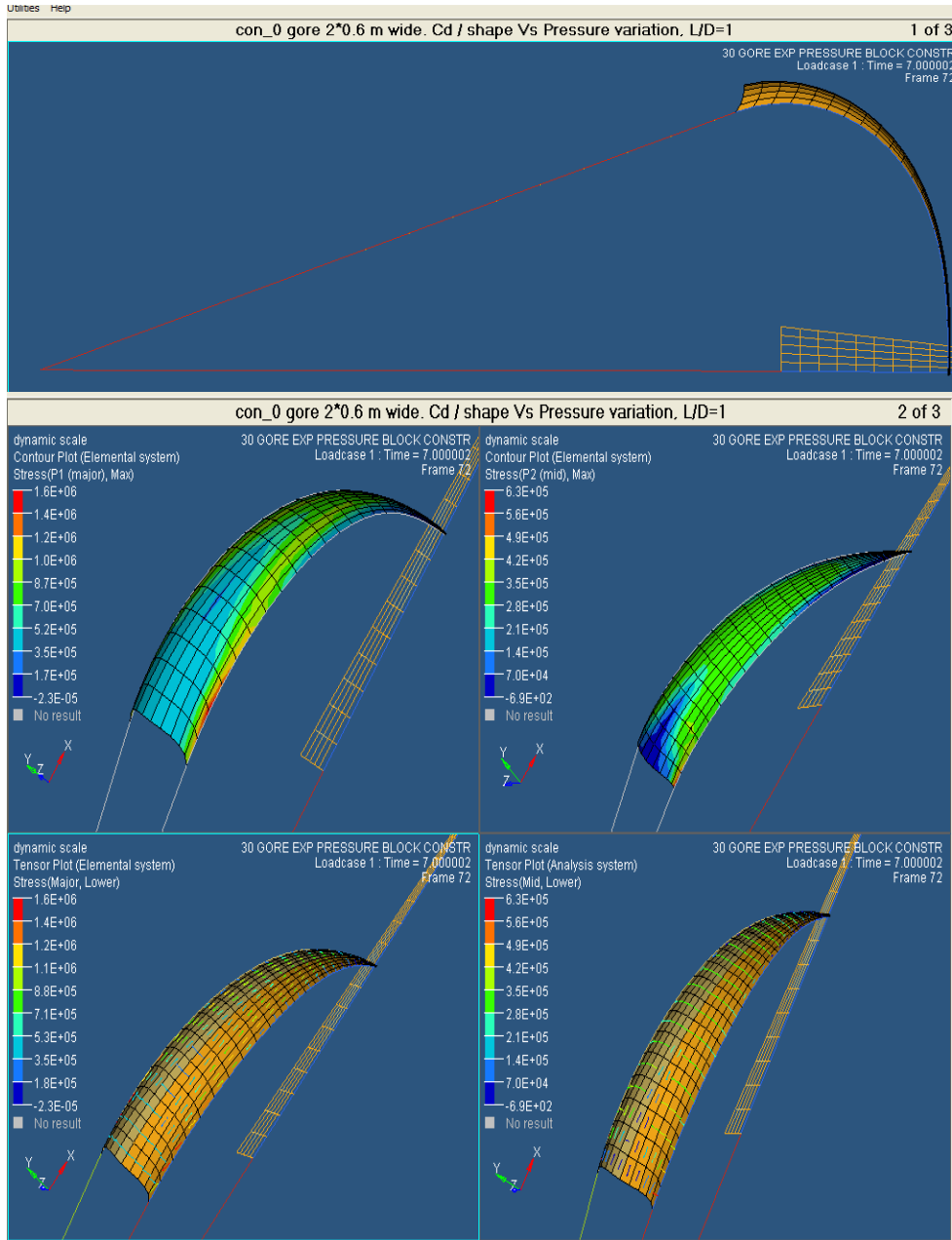


Fig.24

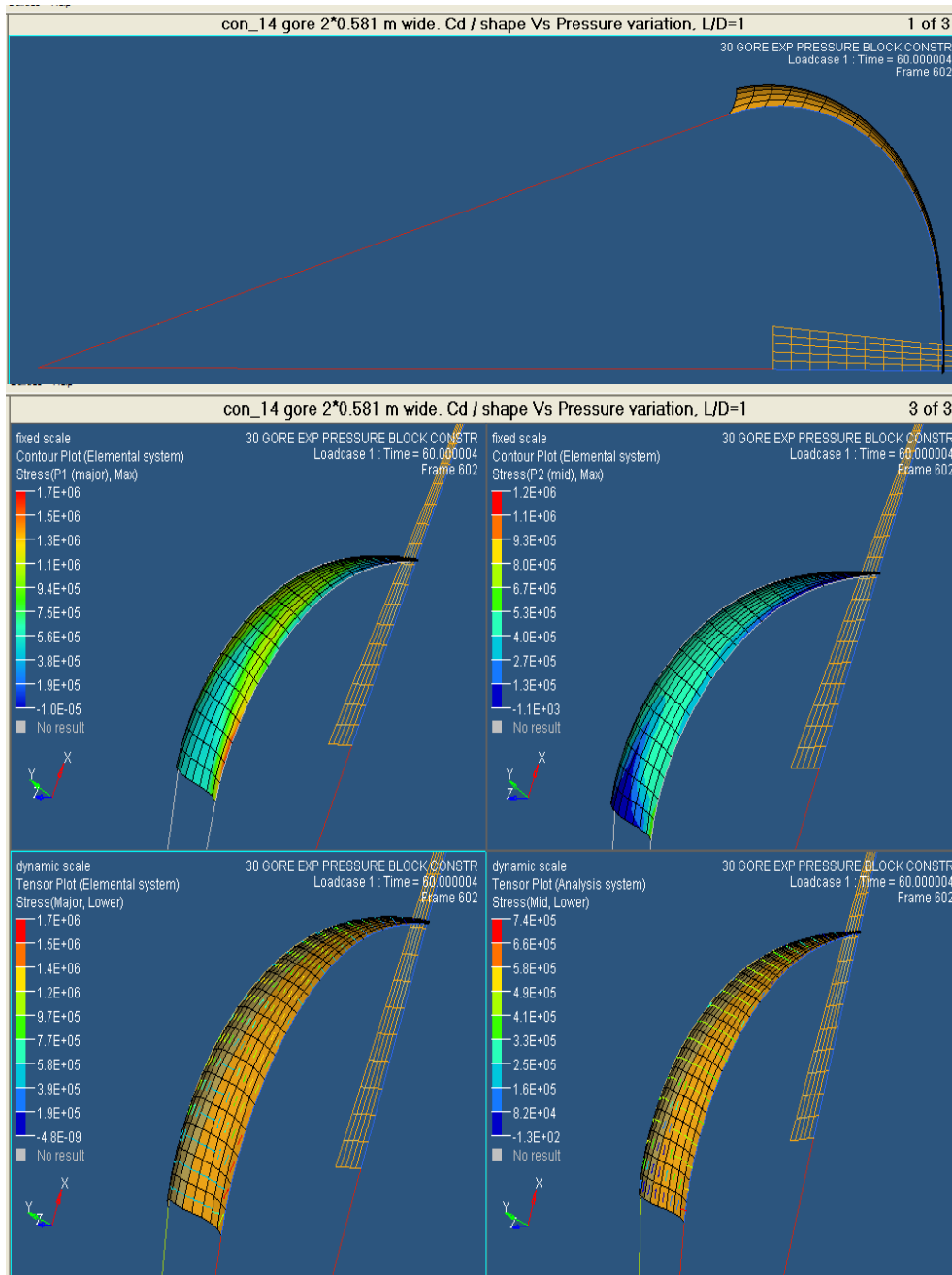


Fig.25

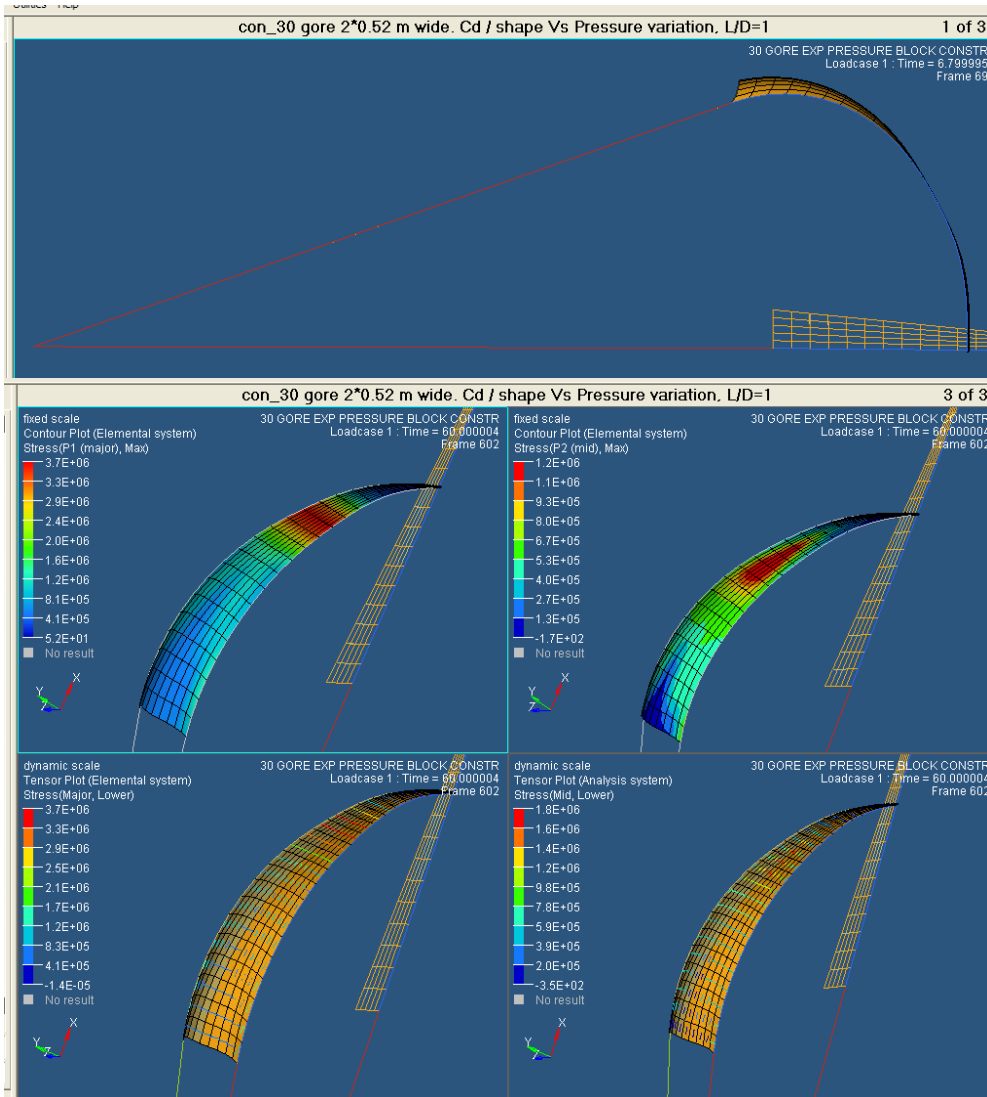


Fig.26

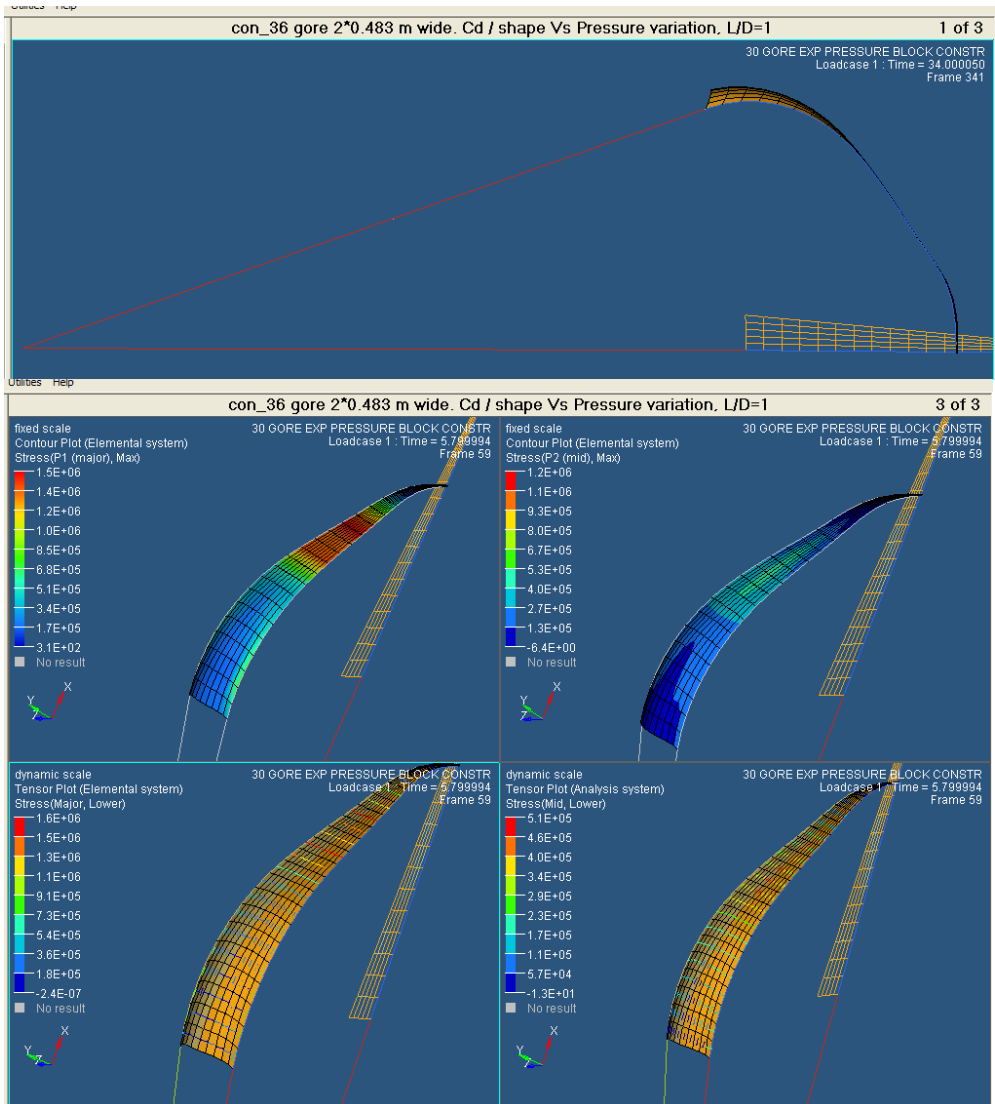


Fig. 27

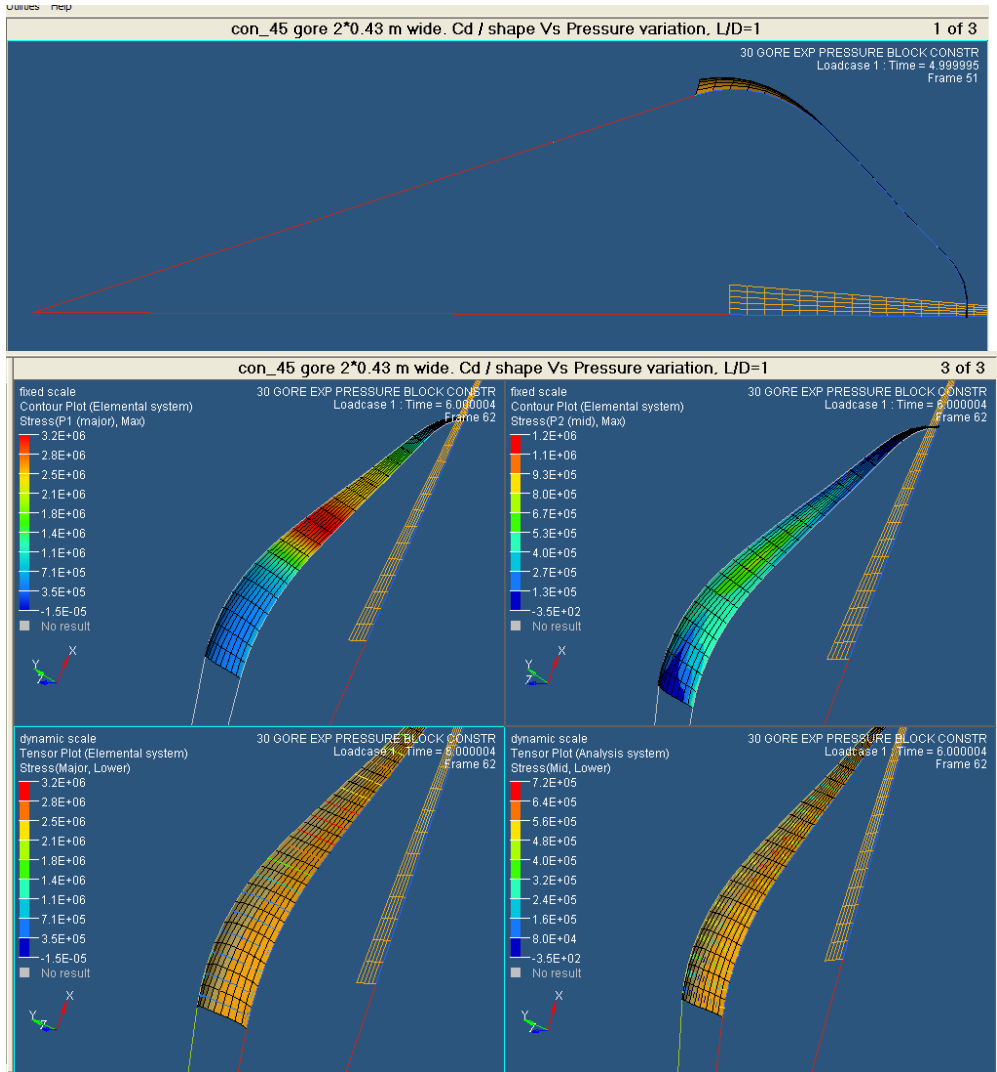


Fig. 28

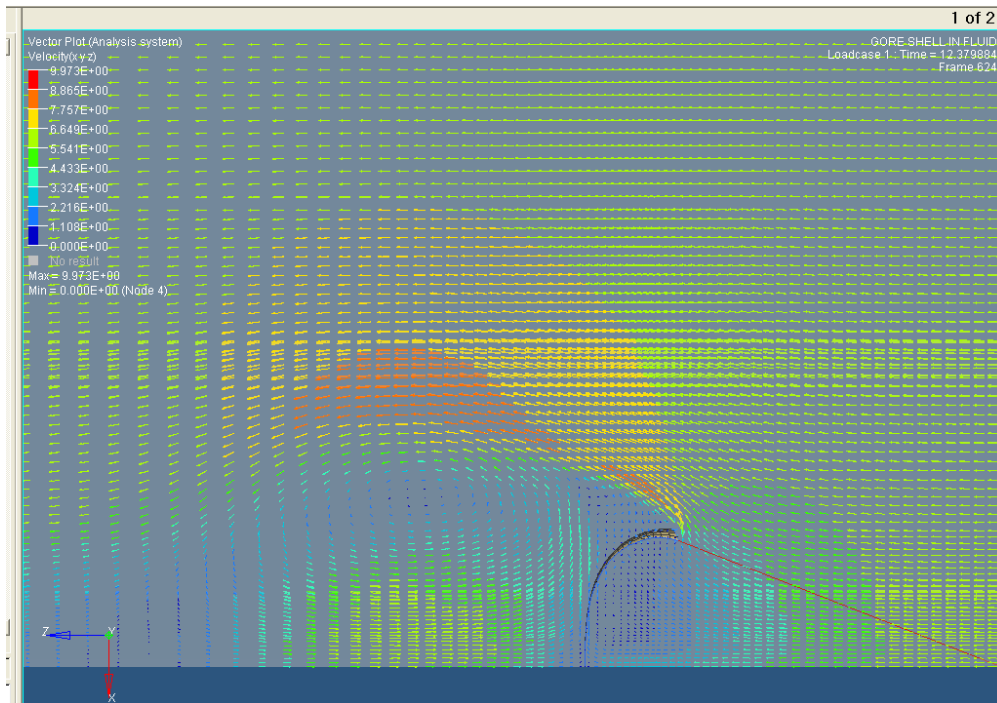


Fig. 29

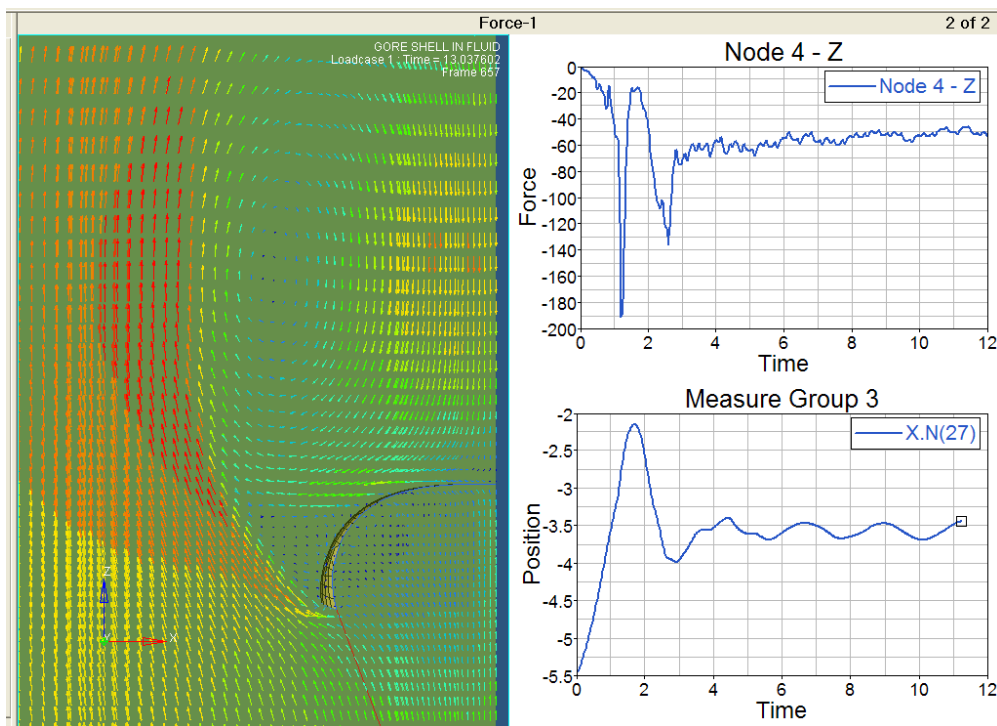


Fig 30